Research Article

Dysregulated expression and distribution of Kif5α in neurites of wobbler motor neurons

Kilian Kürten, Anne-Christin Gude, Aimo Samuel Christian Epplen, Jan Stein, Carsten Theiss, Veronika Matschke[*]

From the Contents

Graphical Abstract

Dysregulation of Kif5α in motor neuronal branches of the Wobbler mouse, a model of amyotrophic lateral sclerosis, may result in abnormal transport of proteins and organells
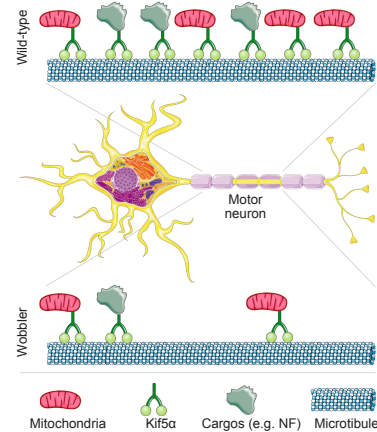
Abstract

Impaired axonal transport has been observed in patients with amyotrophic lateral sclerosis (ALS) and in animal models, suggesting that transport proteins likely play a critical role in the pathological mechanism of ALS. Dysregulation of Kinesin-family-member 5α (Kif5α), a neuron-specific isoform of heavy chain kinesin family, has been described in several neurological disorders, in humans and animal models, including ALS. In this study, we determined Kif5α expression by gene sequencing, quantitative reverse transcription-polymerase chain reaction, and western blot assay in the cervical spinal cord of wobbler mice and immunofluorescence staining in dissociated cultures of the ventral horn. Further, we observed the distribution of Kif5α and mitochondria along motor neuronal branches by confocal imaging. Our results showed that Kif5α expression was greatly dysregulated in wobbler mice, which resulted in altered distribution of Kif5α along motor neuronal branches with an abnormal mitochondrial distribution. Thus, our results indicate that dysregulation of Kif5 and therefore abnormal transport in motor neuronal branches in this ALS model could be causative for several pathological findings at the cellular level, like misallocation of cytoskeletal proteins or organelles like mitochondria.

Key Words: amyotrophic lateral sclerosis; cell culture; kinesin; mitochondria; neurodegeneration; spinal cord; transport

Introduction

Amyotrophic lateral sclerosis (ALS) is a fatal neurodegenerative disease that selectively affects the upper and lower motor neurons in the brain and spinal cord (Kiernan et al., 2011). It leads to ineluctable death within 2–5 years after the disease onset, usually due to respiratory failure (Bruijn et al., 2004). Approximately 5–10% of diagnosed ALS cases are familial with ALS-typical mutations in several genes (Zou et al., 2017). ALS-typical mutations include a loss-of-function mutation in the kinesin family member 5A (KIF5A) gene (Brenner et al., 2018; Nicolas et al., 2018), leading to a disrupted Kif5α C-terminal sequence, potentially affecting the binding of specific cargo proteins (Naruse et al., 2021).

Kif5α is a neuron-specific isoform of a heavy chain kinesin (Aizawa et al., 1992; Niclas et al., 1994; DeBoer et al., 2008). This molecule carries out anterograde transport of proteins and organelles including a vast variety of vesicles and mitochondria from the perikaryon to the periphery (Hirokawa et al., 2010; Kamata et al., 2017). Studies on different model systems show the great importance of Kif5α for the long-distance axonal transport (Uchida et al., 2009; Wang et al., 2019) because mutations or manipulations on the expression of this protein lead to altered kinetics of transport, maldistribution of mitochondria, and subsequently degeneration of neurons (Campbell et al., 2014). Interestingly, impaired axonal transport was shown to be linked to mitochondrial dysfunction (Ferraiuolo et al., 2001; Moser et al., 2013). Kif5α loss-of-function mutations in the C-terminus of the protein have been recently detected in ALS patients (Brenner et al., 2018; Nicolas et al., 2018), indicating a link between mechanisms of altered cytoskeletal dynamics and the disease ALS (Taylor et al., 2016; Chia et al., 2018). Moreover, a decreased survival rate of motor neurons compared to less affected sensory neurons has been shown in Kif5α knockout mice. In particular, mitochondrial transport velocity and axonal growth decrease through the loss of Kif5a, affecting motor neurons more sverely (Karle et al., 2012). Inactivation of Kif5a, via a Cre-mediated

postnatal loss, has been shown to lead to accumulation of neurofilaments (NF), NF-H (high molecular weight), NF-M (medium molecular weight), and NF-L (low molecular weight) in cell bodies of sensory neurons in mice (Xia et al., 2003). Interestingly, both ALS patients and wobbler mice (established animal model of ALS) show an altered distribution of phosphorylated NF in motor neurons, with accumulation at the perikaryon that does not differentiate between moderate and severe disease severity (Manetto et al., 1988; Pernas-Alonso et al., 2001).

In this study, we used the wobbler mouse, which is derived from a C57BL/Fa strain suffering from a spontaneous loss-of-function mutation in the vacuolar protein sorting-associated protein 54 (*Vps54*) gene. The *Vps54* gene encodes for a part of the Golgi-associated retrograde protein (GARP) complex that is involved in retrograde transport processes from the early and late endosomes to the trans-Golgi network (Schmitt-John et al., 2005). Only homozygous wobbler mice develop the wobbler phenotype, which is strikingly similar to that of ALS patients (Boillée et al., 2003; Moser et al., 2013; Ott et al., 2015). Three developmental phases of the disease can be observed in the wobbler mouse. While at presymptomatic phase (postnatal day 0–19 [p0–p19]) no clinical symptoms are obvious, wobbler mice start to show pathological symptoms 20 days after birth (evolutionary phase; p20-p39), beginning with muscle weakness at the front feet and typical head tremor, finally reaching back feet and tail. In addition, these mice are small in size compared to healthy littermates (Boillée et al., 2003; Ott et al., 2015). Finally, at the stable phase (from p40), the wobbler phenotype is fully developed. Remarkably, motor impairment and pathologies such as altered protein patterns that might lead to neuronal cell death occur in the cervical part of the spinal cord at certain phases of the disease without being altered in the lumbar region (Bastone et al., 2009; Moser et al., 2013).

Since compromised axonal transport has been shown both, in ALS patients and in animal models like wobbler mice, these processes are crucial to

Department of Cytology, Institute of Anatomy, Medical Faculty, Ruhr University Bochum, Bochum, Germany
***Correspondence to:** Veronika Matschke, Dr. rer. nat., Veronika.Matschke@rub.de.
https://orcid.org/0000-0001-9717-4485 (Veronika Matschke)

understand the role of transport proteins in the pathomechanisms of ALS (Mitsumoto et al., 1990; Ferraiuolo et al., 2001; Pernas-Alonso et al., 2001; Kiernan et al., 2011; Moser et al., 2013). In the current study, we used the wobbler mouse to investigate the expression of Kif5a, which is involved in the transport of proteins and organelles, like NF and mitochondria, in the cervical spinal cord and more specifically the distribution of this motor protein in motor neurons of the animals at different phases of the disease. Our results may provide a valuable contribution to the understanding of the role of Kif5α in the development and evolution of ALS.

Methods

Animals
All animals were handled in accordance with the standards of the German federal state of North Rhine-Westphalia and the European Communities Council Directive 2010/63/EU on the protection of animals used for scientific purposes. According to current German and European legislation, the removal of organs or cells from vertebrates for scientific purposes is not considered an animal experiment if the animals have not been subject to surgical interventions or invasive treatments prior to sacrifice. Thus, the sacrifice of laboratory animals in this study is not subject to approval and does not have to be confirmed by any committee in Germany.

The mouse strain used was C57BL/Fa carrying the wobbler mutation. The mice were bred and genotyped as previously described (Ott et al., 2015). All mice were kept at a 12-hour day/night cycle in an open cage, in which food and water were available *ad libitum*. Cervical spinal cord tissue (C1–C8) was collected under a microscope at three developmental phases: postnatal day (p) 0, p20, and p40. Four exclusively homozygous couples of wobbler and wild-type mice were sacrificed at each of the three time points for later experiments. Both genders were used.

Quantitative reverse transcription-polymerase chain reaction
Total RNA (tRNA) was obtained from the cervical spinal cord tissue of healthy wild-type and wobbler mice at the time points mentioned above using the NucleoSpin miRNA Kit (Macherey-Nagel, Düren, Germany, Cat# 740971) in accordance with the original manufacturer protocol. cDNA was synthesized using Reverse Transcription System (Promega, Madison, WI, USA, Cat# A3500), as described in the manufacturer protocol using 1 µg tRNA and oligo(dT) primer. cDNA was stored at −20°C until use. Standard quantitative reverse transcription-polymerase chain reaction (qRT-PCR) was performed on a CFX96 Real-Time PCR Detection System (Bio-Rad, Hercules, CA, USA) using GoTag qPCR Master Mix (Cat# A6001, Promega), 100 ng of cDNA per reaction, and 0.7 µM primer. The primer sequences for *Gapdh* were sense: 5′-GGA GAA ACC TGC CAA GTA TGA-3′, and antisense: 5′-TCC TCA GTG TAG CCC AAG A-3′. The primer sequences for Kif5α were sense: 5′-GAA GGA GAA GGA GAA GAC CAA G-3′, and antisense: 5′-CAG TCT CAG GCA CAT TCT CTC-3′. After each PCR run (see the manufacture protocol for "reaction protocols"). Melting curves regarding single PCR products were plotted. Expression levels of Kif5α and the housekeeping gene *Gapdh* were analyzed in triplicate. The $2^{-\Delta\Delta CT}$ method (Livak and Schmittgen, 2001) was used to analyze obtained data.

Western blot assay
Western blot assay was performed as previously described (Röderer et al., 2018). In brief, protein was isolated from cervical spinal cord tissue with RIPA buffer (150 mM NaCl, 20 mM Tris-HCl, 0.1% sodium dodecyl sulfate, 1% Triton-X100, 1% sodium deoxycholate, 1 mM Na2EDTA). The concentrations of obtained protein were measured using the Pierce™ BCA Protein Assay Kit (Thermo Fisher Scientific, Waltham, MA, USA, Cat# 23225). 50 µg of total protein per lane was used. Proteins were separated by sodium dodecyl sulfate-polyacrylamide gel electrophoresis and blotted onto nitrocellulose membranes. Following a blocking procedure at room temperature in 1× phosphate buffered saline (PBS) containing 1% RotiBlock (Roth, Karlsruhe, Deutschland, Cat# A151) for a minimum of 1 hour, primary rabbit polyclonal IgG anti-Kif5α antibody (1:500; Thermo Fischer Scientific, Cat# PA5-29820, RRID: AB_2547294) and secondary horseradish peroxidase-conjugated goat anti-rabbit IgG antibody (1:5000; Santa Cruz Biotechnology, Dallas, TX, USA, Cat# sc-2054, RRID: AB_631748) were used to detect Kif5α. To detect control protein actin, primary mouse polyclonal IgG anti-β-actin antibody (1:100; Sigma-Aldrich, St. Louis, MO, USA, Cat# A-2668, RRID: AB_258014) and secondary horseradish peroxidase-conjugated donkey anti-mouse IgG antibody (1:5000; Santa Cruz Biotechnology, Cat# sc-2314, RRID: AB_641170) were used. Protein bands were visualized with Western Blotting Luminol Reagent (Santa Cruz Biotechnology, Cat# sc-2048). The band intensity was quantified by arithmetic analysis using the ImageJ 1.53f51 software (U.S. National Institutes of Health, Bethesda, MD, USA). Data were normalized to actin. Normalized values of wobbler samples were compared with normalized wild-type samples at each phase of age and displayed as a percentage in a bar chart.

Molecular cloning and sequencing of mouse Kif5α
cDNA of homozygous wild-type and wobbler spinal cord was obtained as described above and used for sequencing. The sense primer sequences used are as follows: 5′-AGA GCT GGT TTA GTG AAC CG-3′, 5′-TGG ATG TGA TCG ATG AGG GG-3′, 5′-GAG AAC GAT GCT GCG AAG G-3′, 5′-AAG ACA AGG AGC CAG ACA CA-3′, 5′-GTA TCA GCT ACA CCA ACA AC-3′ and 5′-CAC GCT CAT GTT TGG ACA G-3′. The homozygous wild-type and wobbler sequences were compared with the published sequence NM_001039000.4 with MView 1.63 (Brown et al., 1998; **Additional Figure 1**).

Dissociated cell culture of the ventral horn of the spinal cord
The dissociated spinal cord cell cultures were cultivated as previously described (Zwilling et al., 2020). In brief, the spinal cord was isolated at the age of p40. The meninges were carefully plucked off and the anterior horn was separated from the posterior horn. The anterior horn was chopped into small pieces. The tissue pieces were digested with papain (36 U/mL papain) isolation medium (self-prepared; 0.5 mM GlutaMax, 100 U/mL penicillin/streptomycin, 2% B27 supplement in Hibernate A) for 10 minutes at 37°C. After trituration of the tissue, the isolated cells were separated by density gradient centrifugation on an OptiPrep™ (PROGEN Biotechnik GmbH, Heidelberg, Germany, Cat# 1114542) as previously described (Brewer and Toricelli, 2007). The cells from fractions 2 and 3 were pelletized by centrifugation (244 × *g* for 6 minutes at 10°C) and plated in motor neuron feeding medium [self-prepared; 30% C2C12 myocyte-conditioned medium (Zwilling et al., 2020), 0.5 mM glutamine, 100 U/mL penicillin/streptomycin, 2% B27 supplement, 125 mM cAMP, 1 ng/mL brain-derived neurotrophic factor (BDNF), 0.1 ng/mL glial cell line-derived neurotrophic factor (GDNF) in Neurobasal A] at a density of 70,000 cells per well onto poly-D-lysine (50 µg/mL) coated cover glasses. The cells were cultivated *in vitro* for 10 days at 37°C and 5% CO_2 with medium change with motor neuron feeding medium after 2–3 days.

Immunofluorescence staining and confocal laser scanning microscopy
To investigate the distribution of Kif5α along the motor neuronal neurites, dissociated motor neuronal cell cultures were fixed after 10 days *in vitro* with 4% paraformaldehyde (PFA) in PBS for 10 minutes at room temperature. For immunostaining, cultures were permeabilized with 0.3% Triton-X 100 in PBS for 10 minutes before blocking with 5% goat serum in PBS for 30 minutes at room temperature. The cells were further incubated with the primary antibodies (1:500, mouse Tuj1 antibody, R&D systems, Minneapolis, MN, USA, Cat# MAB1195, RRID: AB_357520; 1:200, rabbit Kif5α antibody, Thermo Fischer Scientific, Cat# PA5-29820, RRID: AB_2547294) at 4°C overnight. The samples were then reacted with secondary antibodies for 2 hours at room temperature (1:400, anti-mouse-AlexaFluorPlus594, Thermo Fisher Scientific, Cat# A32744, RRID: AB_2762826; 1:300, anti-rabbit-AlexaFluor488, Thermo Fisher Scientific, Cat# A11008, RRID: AB_143165). Nuclei were stained with 4′,6-diamidino-2-phenylindole (DAPI, 1 µg/mL; Sigma-Aldrich, Cat# D9542). Finally, slides were rinsed in PBS and cover slipped in fluoromount (Cat# F4680, Sigma-Aldrich).

To investigate the distribution of mitochondria in motor neuronal cells, CellTracker (10 µM, Thermo Fisher Scientific, Cat# C7025) and MitoTracker (100 nM, Thermo Fisher Scientific, Cat# M7512) were used. Samples were imaged using an inverted confocal Laser Scanning Microscope (LSM 800, Carl Zeiss Microscopy GmbH, Jena, Germany) equipped with the respective filter sets in combination with a 40× objective (Plan-Apochromat 40×/1.4 Oil, Carl Zeiss Microscopy GmbH). The settings of the recordings were not changed between the individual phenotypes. Secondary antibodies were tested for specificity and showen no unspecific binding.

Analysis of Kif5α immunofluorescence staining
Tuj1-positive axons of motor neuronal cells were measured using Zeiss ZEN blue software (Carl Zeiss Microscopy GmbH, Jena, Germany). Within each axon, Kif5α positive signals were evaluated. To compare the number of kinesins between wild-type and wobbler samples, Kif5α positive signals were normalized to the length of the axon. The counting was performed in a double assessment in a blind study. To investigate the distribution of kinesin molecules along the axon, the length of each axon was set to 100% and the distribution of Kif5α signal counts was compared between the genotypes.

Statistical analysis
Data were statistically analyzed with GraphPad Prism 6.1 software (GraphPad Software, San Diego, CA, USA). The Kolmogorov-Smirnov normality test was used to confirm normal distribution. Data are expressed as means ± SEM. Data were tested for significance using the Student's *t*-test. Results with $P < 0.05$ were considered statistically significant.

Results

Dysregulated Kif5α expression in cervical spinal cord of symptomatic wobbler mice
We utilized qRT-PCR and western blotting to detect possible dysregulation of Kif5α expression at mRNA and protein levels during three developmental phases of wild-type and wobbler mice. Gene expression of *Kif5α* was dysregulated at p20 and p40 (**Figure 1A**). At p0, there was no significant difference in gene expression level between wild-type and wobbler mice (**Figure 1A**). A significant upregulation of *Kif5α* mRNA was found to be present in the cervical part of the spinal cord of wobbler mice at p20, whereas a highly significant downregulation was observed at p40, compared with wild-type mice (**Figure 1A**). These findings were confirmed by blotting performed at p40 at protein level. However, at p20, no dysregulation of Kif5α protein level was shown (**Figure 1B** and **C**).

No mutations in *Kif5α* gene of wobbler mice
To rule out a *Kif5α* mutation as a cause for possible dysregulation in wobbler mice, we performed sequencing of *Kif5α* in wild-type and wobbler mice. There was no difference in the sequence of *Kif5α* between homozygous wild-type and wobbler sequences (**Additional Figure 1**). It can therefore be excluded that a mutation is causative for the dysregulation observed at the mRNA and protein levels in the cervical spinal cord of wobbler mice.
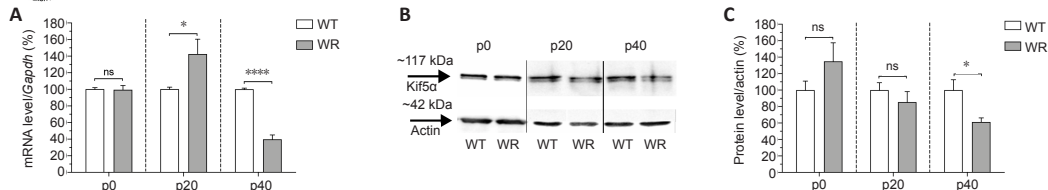
Figure 1 │ Age-dependent differential expression of Kif5α in the cervical spinal cord of the wobbler mouse.
(A) Expression levels of *Kif5α* mRNA from presymptomatic to stationary phase of wild-type (WT) and wobbler (WR) cervical spinal cord were determined by quantitative real-time PCR using four samples for each genotype and stage. A significant upregulation of *Kif5α* was detected at the evolutionary (p20) phase and a significant downregulation at stationary (p40) phase of wobbler mice. For relative quantification of *Kif5α* expression, the $2^{-\Delta\Delta Ct}$ method was conducted using the housekeeping gene *Gapdh* for normalization. Data are provided as the mean ± SEM. Data were tested for significance using Student's *t*-test. Significant differences are indicated by *$P < 0.05$, ****$P < 0.0001$, ns = not significant; $n = 4$. (B) Representative western blot of Kif5α protein expression levels in WT and WR cervical spinal cord at three developmental phases. Actin was used as a control protein. Intensity values of Kif5α in WT cervical spinal cord were normalized to actin and were compared with WT mice. (C) Semi-quantitative analysis of Kif5α protein expression level in the cervical spinal cord from presymptomatic to stationary phase of WT and WR. Only at p40, a significant downregulation of Kif5α was detected. Data are provided as the mean ± SEM. Differences were tested using Student's *t*-test. Significant differences are indicated by *$P < 0.05$, ns = not significant; $n = 5$–11.

Altered Kif5α signals in the neurites of wobbler motor neurons

Due to their long axons, motor neurons are extremely dependent on axonal transport. As they are specifically affected by ALS, they are a very important target for further investigation. Since dysregulation of Kif5α expression in clinical wobbler mice was dysregulated at p40, we investigated the possible intracellular expression differences caused by this dysregulation using immunofluorescence staining and confocal laser microscopy. We found significantly lower kinesin spots in wobbler motor neuronal neurites compared with wild-type neurites (**Figure 2**). The signal distribution of Kif5α in wild-type and wobbler neurites generally followed the same trend, with the neurites of wobbler mice uniformly showing fewer kinesin spots and accumulations (**Figure 3**). It becomes obvious that kinesin signals could be detected as accumulations of molecules along the motor neuronal neurite of wild-type mice. The number of signals in the neurites of wobbler motor neurons was generally lower and accumulations occurred in a smaller quantity and did not reach the growth cone. Since existing literature suggests that Kif5α is important for mitochondrial transport and distribution, we performed experiments to qualitatively investigate the distribution of mitochondria in motor neurons of both genotypes at p40 (**Additional Figure 2**). While mitochondria in wild-type motor neurons are distributed relatively homogeneously over all branches with accumulations along the neurites (**Additional Figure 2A**), first hints could be gained on an altered distribution of mitochondria in Wobbler cells (**Additional Figure 2B**). However, these results still need to be supported by further studies.
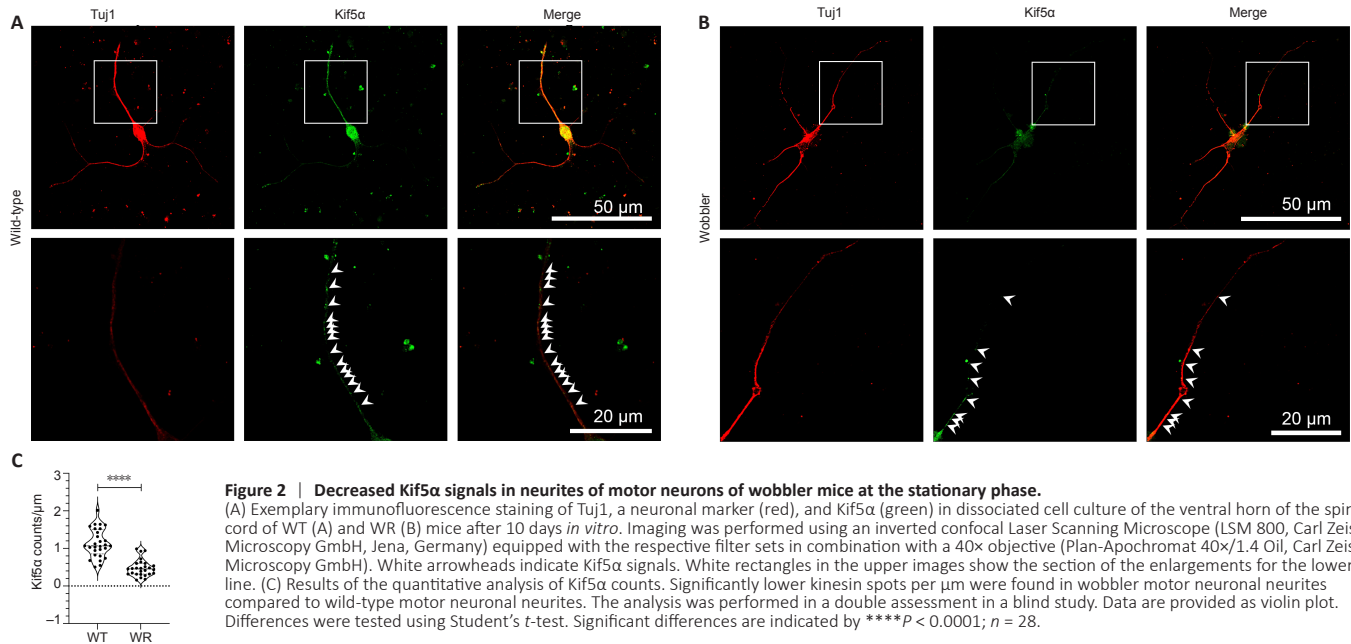

Figure 2 │ Decreased Kif5α signals in neurites of motor neurons of wobbler mice at the stationary phase.
(A) Exemplary immunofluorescence staining of Tuj1, a neuronal marker (red), and Kif5α (green) in dissociated cell culture of the ventral horn of the spinal cord of WT (A) and WR (B) mice after 10 days *in vitro*. Imaging was performed using an inverted confocal Laser Scanning Microscope (LSM 800, Carl Zeiss Microscopy GmbH, Jena, Germany) equipped with the respective filter sets in combination with a 40× objective (Plan-Apochromat 40×/1.4 Oil, Carl Zeiss Microscopy GmbH). White arrowheads indicate Kif5α signals. White rectangles in the upper images show the section of the enlargements for the lower line. (C) Results of the quantitative analysis of Kif5α counts. Significantly lower kinesin spots per μm were found in wobbler motor neuronal neurites compared to wild-type motor neuronal neurites. The analysis was performed in a double assessment in a blind study. Data are provided as violin plot. Differences were tested using Student's *t*-test. Significant differences are indicated by ****$P < 0.0001$; $n = 28$.
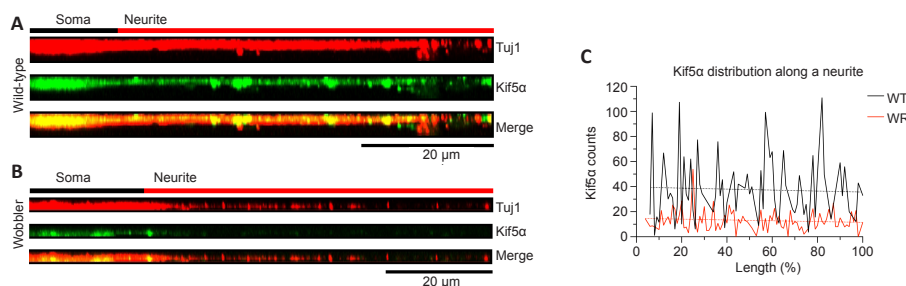

Figure 3 │ Altered signals of kinesin spots in motor neuronal neurites of wobbler mice.
(A, B) Exemplary X–Z projection of immunofluorescence staining of Tuj1, a neuronal marker (red), and Kif5α (green) in dissociated cell culture of the ventral horn of the spinal cord of WT (A) and WR (B) mice after 10 days *in vitro*. Neurites of wobbler motor neurons accumulated in a small quantity and did not reach the growth cone. Imaging was performed using an inverted confocal Laser Scanning Microscope (LSM 800, Carl Zeiss Microscopy GmbH, Jena, Germany) equipped with the respective filter sets in combination with a 40× objective (Plan-Apochromat 40×/1.4 Oil, Carl Zeiss Microscopy GmbH). (C) Distribution of kinesin signals along the neurites was analyzed by setting the length of each neurite to 100% and distribution of Kif5α signal counts was compared between the genotypes. Dotted line represents a linear regression line of the distribution of kinesin signals along the neurite.

Discussion

Impaired axonal transport plays a crucial role in the pathogenesis of ALS and various ALS models (Mitsumoto et al., 1990; Taylor et al., 2016; Brenner et al., 2018; Chia et al., 2018; Nicolas et al., 2018). The neuron-specific kinesin subunit Kif5α is therefore of special interest for investigation of ALS, a degenerative disease of the motor neuron system.

It is known that impairment of Kif5α leads to different pathological conditions like, (I) transport disorders and NF accumulation (Xia et al., 2003), (II) decrease in mitochondrial transport quantity and velocity (Karle et al., 2012; Wang et al., 2019), and (III) persistence of mitochondria in the main stem of the axons combined with a general intracellular decrease of mitochondria (Campbell et al., 2014; Stein et al., 2021). Therefore, Kif5α seems to be not only part of a potentially impaired neuronal intracellular transport but also a reason for other intracellular impairments such as NF accumulation and an impaired mitochondrial distribution process.

Our results reveal that wobbler mice did not show any dysregulation of Kif5α expression at birth. It can be assumed that the effects of the wobbler mutation at birth had not yet caused extensive cellular impairments, thus not altering the expression levels of Kif5α. Many of the factors investigated in wobbler mice also showed no differences in expression at this stage of age (Pernas-Alonso et al., 2001; Moser et al., 2013; Saberi et al., 2016). These findings correlate with the fact that newborn wobbler mice did not show any symptoms (Boillée et al., 2003).

At p20, we showed that wobbler mice still did not show severe symptoms, however, at the molecular level, a significant upregulation of Kif5α mRNA was detected compared to wild-type mice. Nevertheless, the protein level was not altered. There could be several reasons for this phenomenon. On one hand, it could be a compensation reaction in which a reduced protein level was to be balanced by increased mRNA expression. On the other hand, dysregulated miRNAs might also play a role in the translation control of Kif5α, as have been shown for other molecules in the wobbler mouse (Klatt et al., 2019; Rohm et al., 2019). A recent study could show an upregulation of Kif5 via miRNA when distal axon growth is inhibited through chondroitin sulfate proteoglycans (Li et al., 2019). Similar upregulation might be induced by impaired pathways due to the wobbler mutation.

In the current study, at the symptomatic phase, a significant downregulation of Kif5α was shown at both mRNA and protein levels, although Kif5α does not reach the growth cone either. At this point, cellular impairment was observed in motor neurons (Boillée et al., 2003), suggesting a correlation between the continuous aggravation of Kif5α synthesis and motor neuron degeneration.

We showed reduced expression of Kif5α in the cervical spinal cord which was preceded by increased mRNA expression during the evolutionary phase (p20). Since Kif5α in cerebrospinal fluid has already been used as an experimental biomarker to monitor the severity of multiple sclerosis (Hares et al., 2021), similar trials could be conducted among family members of patients with familial ALS. In this way, it might be possible to detect pathological changes before symptoms appear and initiate treatment at an early phase. Even though the wobbler mutation affects the process of vesicle tethering ubiquitously and is causing cellular impairment not exclusively in motor neurons, they are especially affected (Moser et al., 2013). Since motor neurons are extremely large cells, reaching over extremely long distances, dysregulation of the neuron exclusive subunit Kif5α can affect them more severely, similar to the decrease of motor neurons in Kif5α knockout mice (Karle et al., 2012).

Our results showed a reduced expression level of Kif5α in spinal cord of wobbler mice and abnormal Kif5α distribution that did not extend into the growth cone. Accordingly, our very first results showed a decreased quantity of mitochondria along the neurites of Wobbler motor neurons, which also did not reach the distal parts of the observed branches. We speculate that the deficiency of Kif5α might be responsible for a maldistribution and reduced quantity of mitochondria in motor neuronal branches. This is in line with the observations described above in the Kif5α knockout model suffering from the generally reduced number of mitochondria and their persistence at the stem axon (Campbell et al., 2014). Dysfunctional mitochondria are found in wobbler mice, which further deteriorate in the stable phase (Xu et al., 2001; Dave et al., 2003). It is possible that mitochondrial dysfunction is caused by maldistribution due to impaired Kif5α regulation, possibly exacerbated by the reduced rate of mitochondrial transport, which was not investigated in this study, but was described in Kif5α knockout models (Karle et al., 2012). Since mitochondria enable the axon to extend, branch, and regenerate (Smith et al., 2019), their decline in the neuronal periphery and growth cone was likely to further deteriorate neurodegeneration.

In addition to mitochondria, other cellular components may also suffer from Kif5α deficiency, such as the cytoskeleton. NF are essential for axonal structural stability and their radial growth (Yuan et al., 2012) and provide as part of the cytoskeleton structural stability to the neuron and its organelles (Yuan et al., 2017). If NF are no longer transported along the axon due to a malfunction or an actual decrease of Kif5α in the neuron periphery, they have a higher risk of degeneration (Yuan et al., 2012). In particular, the stability of neurons with large axons, such as motor neurons, is at risk. Recent studies show that detection of the light subunit of NF-L in cerebrospinal fluid or plasma is indicative of axonal damage and neuronal cell death (Brureau et al., 2017) in ALS and Alzheimer's disease (Loeffler et al., 2020). In this context,

the increase in NF-L in cerebrospinal fluid reliably indicates ALS progression (Loeffler et al., 2020; Sun et al., 2020).

An accumulation of NF in motor neurons was described as a hallmark of ALS in humans (Lu et al., 2011) and was shown in Kif5α knockout models (Xia et al., 2003; Karle et al., 2012). Kif5α is of particular importance for the transport of these cytoskeletal proteins in neurites (Uchida et al., 2009). In consequence, the decrease of Kif5α quantity and its altered distribution along the neurites of wobbler motor neurons at the stationary phase shown in this study likely affect NF distribution. Our findings therefore might explain the accumulation of NF in cell bodies and axonal swellings of Kif5α knockout models (Karle et al., 2012; Nicolas et al., 2018) and at the perikaryon of neurons in wobbler mice (Ott et al., 2017).

We showed for the first time that Kif5α was not dysregulated due to a mutation in the corresponding KIF5α gene in wobbler mice. However, its dysregulation may be a critical secondary effect of the wobbler mutation in the Vps54 gene, although a link between Vps54 functionality and dysregulation of Kif5α remains elusive. This secondary effect may lead to an impaired distribution of organelles such as mitochondria in neurites of motor neurons (**Additional Figure 2**) and might also be responsible for the known accumulation of NF in wobbler mice and ALS patients, leading to neurodegeneration. A recent study on a Charcot Marie Tooth model revealed that compensation for the loss of Kif5α dependent cargo inhibited axonal degeneration (Fukuda et al., 2021). If Kif5α impairments are a common denominator of motor neuron degeneration despite different origins, new therapeutic opportunities for ALS can be created by compensating the loss of function of Kif5α.

Our data showed for the first time dysregulated expression and distribution of Kif5α in wobbler motor neurons. Furthermore, we could demonstrate that mitochondria, transported in particular by Kif5α, are differentially distributed in motor neurons of wobbler mice. Thus, our results indicate that dysregulation of Kif5α and therefore abnormal transport in motor neuronal branches in the wobbler mouse model of ALS may be causative for many pathological findings at the cellular level, e.g. a misallocation or abnormal distribution of cytoskeletal proteins or organelles such as mitochondria. Such a misdistribution of important cargos, especially mitochondria, can result in abnormal metabolic function and further degeneration. Accordingly, our results are in line with current publications that reveal Kif5 to cause certain forms of fALS (Brenner et al., 2018) or to be associated with ALS emphasizing the importance of Kif5 as a significant target for further research (Nicolas et al., 2018).
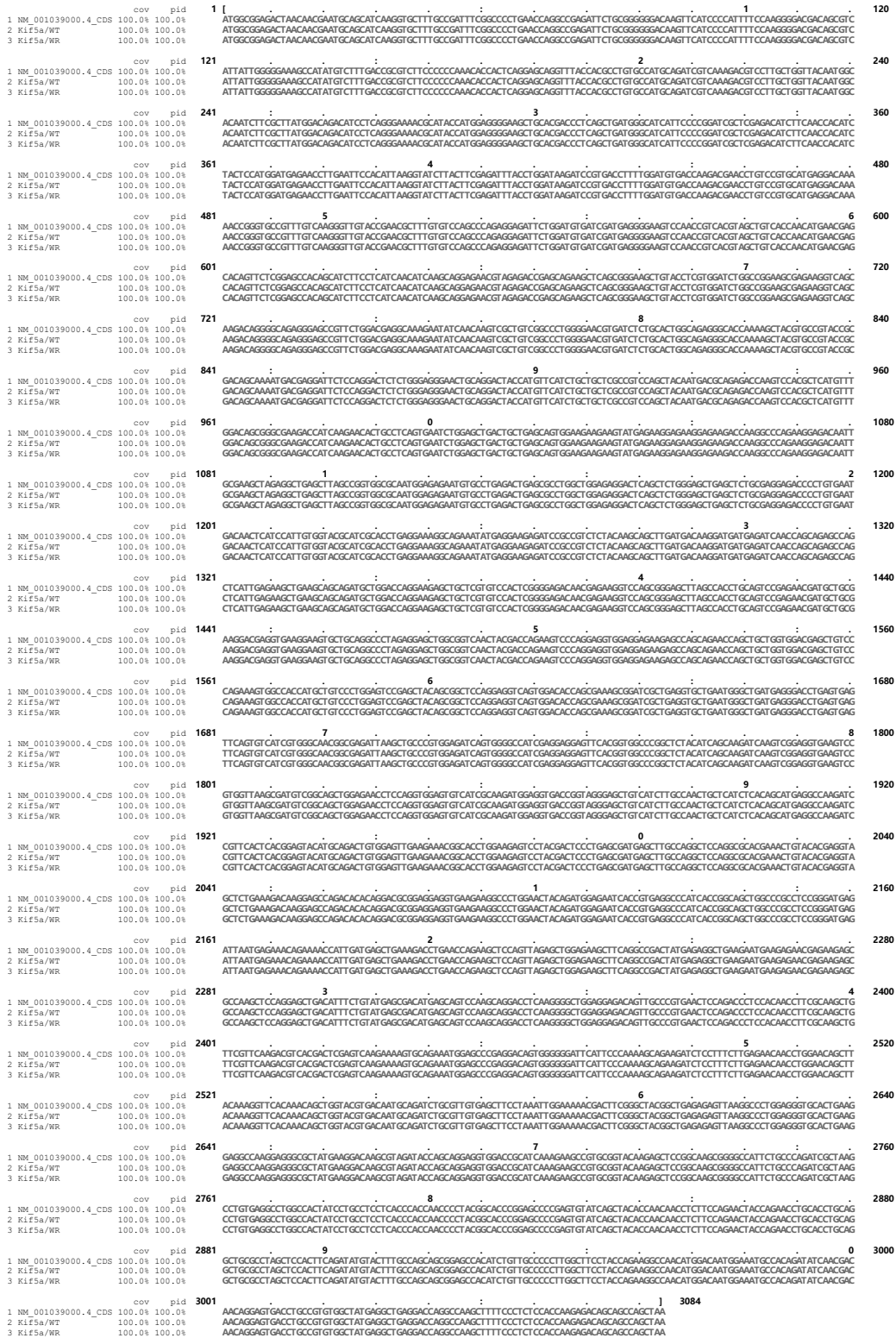
Additional files:
Additional Figure 1: Multiple sequence alignment of WT, WR, and published Kif5α sequence NM_001039000.4.
Additional Figure 2: Altered distribution of mitochondria in motor neuronal neurites of wobbler mice.

References

Aizawa H, Sekine Y, Takemura R, Zhang Z, Nangaku M, Hirokawa N (1992) Kinesin family in murine central nervous system. J Cell Biol 119:1287-1296.

Bastone A, Fumagalli E, Bigini P, Perini P, Bernardinello D, Cagnotto A, Mereghetti I, Curti D, Salmona M, Mennini T (2009) Proteomic profiling of cervical and lumbar spinal cord reveals potential protective mechanisms in the wobbler mouse, a model of motor neuron degeneration. J Proteome Res 8:5229-5240.

Boillée S, Peschanski M, Junier MP (2003) The wobbler mouse: a neurodegeneration jigsaw puzzle. Mol Neurobiol 28:65-106.

Brenner D, Yilmaz R, Müller K, Grehl T, Petri S, Meyer T, Grosskreutz J, Weydt P, Ruf W, Neuwirth C, Weber M, Pinto S, Claeys KG, Schrank B, Jordan B, Knehr A, Günther K, Hübers A, Zeller D, Kubisch C, et al. (2018) Hot-spot KIF5A mutations cause familial ALS. Brain 141:688-697.

Brewer GJ, Torricelli JR (2007) Isolation and culture of adult neurons and neurospheres. Nat Protoc 2:1490-1498.

Brown NP, Leroy C, Sander C (1998) MView: a web-compatible database search or multiple alignment viewer. Bioinformatics 14:380-381.

Bruijn LI, Miller TM, Cleveland DW (2004) Unraveling the mechanisms involved in motor neuron degeneration in ALS. Annu Rev Neurosci 27:723-749.

Brureau A, Blanchard-Bregeon V, Pech C, Hamon S, Chaillou P, Guillemot JC, Barneoud P, Bertrand P, Pradier L, Rooney T, Schussler N (2017) NF-L in cerebrospinal fluid and serum is a biomarker of neuronal damage in an inducible mouse model of neurodegeneration. Neurobiol Dis 104:73-84.

Campbell PD, Shen K, Sapio MR, Glenn TD, Talbot WS, Marlow FL (2014) Unique function of Kinesin Kif5A in localization of mitochondria in axons. J Neurosci 34:14717-14732.

Chia R, Chiò A, Traynor BJ (2018) Novel genes associated with amyotrophic lateral sclerosis: diagnostic and clinical implications. Lancet Neurol 17:94-102.

Dave KR, Bradley WG, Pérez-Pinzón MA (2003) Early mitochondrial dysfunction occurs in motor cortex and spinal cord at the onset of disease in the Wobbler mouse. Exp Neurol 182:412-420.

DeBoer SR, You Y, Szodorai A, Kaminska A, Pigino G, Nwabuisi E, Wang B, Estrada-Hernandez T, Kins S, Brady ST, Morfini G (2008) Conventional kinesin holoenzymes are composed of heavy and light chain homodimers. Biochemistry 47:4535-4543.

Ferraiuolo L, Kirby J, Grierson AJ, Sendtner M, Shaw PJ (2001) Molecular pathways of motor neuron injury in amyotrophic lateral sclerosis. Nat Rev Neurol 7:616-630.

Fukuda Y, Pazyra-Murphy MF, Silagi ES, Tasdemir-Yilmaz OE, Li Y, Rose L, Yeoh ZC, Vangos NE, Geffken EA, Seo HS, Adelmant G, Bird GH, Walensky LD, Marto JA, Dhe-Paganon S, Segal RA (2021) Binding and transport of SFPQ-RNA granules by KIF5A/KLC1 motors promotes axon survival. J Cell Biol 220:e202005051.

Hares K, Kemp K, Loveless S, Rice CM, Scolding N, Tallantyre E, Robertson N, Wilkins A (2021) KIF5A and the contribution of susceptibility genotypes as a predictive biomarker for multiple sclerosis. J Neurol 268:2175-2184.

Hirokawa N, Niwa S, Tanaka Y (2010) Molecular motors in neurons: transport mechanisms and roles in brain function, development, and disease. Neuron 68:610-638.

Kamata H, Tsukasaki Y, Sakai T, Ikebe R, Wang J, Jeffers A, Boren J, Owens S, Suzuki T, Higashihara M, Idell S, Tucker TA, Ikebe M (2017) KIF5A transports collagen vesicles of myofibroblasts during pleural fibrosis. Sci Rep 7:4556.

Karle KN, Möckel D, Reid E, Schöls L (2012) Axonal transport deficit in a KIF5A(-/-) mouse model. Neurogenetics 13:169-179.

Kiernan MC, Vucic S, Cheah BC, Turner MR, Eisen A, Hardiman O, Burrell JR, Zoing MC (2011) Amyotrophic lateral sclerosis. Lancet 377:942-955.

Klatt CL, Theis V, Hahn S, Theiss C, Matschke V (2019) Deregulated miR-29b-3p correlates with tissue-specific activation of intrinsic apoptosis in an animal model of amyotrophic lateral sclerosis. Cells 8:1077.

Li C, Zhang Y, Levin AM, Fan BY, Teng H, Ghannam MM, Chopp M, Zhang ZG (2019) Distal axonal proteins and their related miRNAs in cultured cortical neurons. Mol Neurobiol 56:2703-2713.

Livak KJ, Schmittgen TD (2001) Analysis of relative gene expression data using real-time quantitative PCR and the 2(-Delta Delta C(T)) Method. Methods 25:402-408.

Loeffler T, Schilcher I, Flunkert S, Hutter-Paier B (2020) Neurofilament-light chain as biomarker of neurodegenerative and rare diseases with high translational value. Front Neurosci 14:579.

Lu CH, Kalmar B, Malaspina A, Greensmith L, Petzold A (2011) A method to solubilise protein aggregates for immunoassay quantification which overcomes the neurofilament "hook" effect. J Neurosci Methods 195:143-150.

Manetto V, Sternberger NH, Perry G, Sternberger LA, Gambetti P (1988) Phosphorylation of neurofilaments is altered in amyotrophic lateral sclerosis. J Neuropathol Exp Neurol 47:642-653.

Mitsumoto H, Ferut AL, Kurahashi K, McQuarrie IG (1990) Impairment of retrograde axonal transport in wobbler mouse motor neuron disease. Muscle Nerve 13:121-126.

Moser JM, Bigini P, Schmitt-John T (2013) The wobbler mouse, an ALS animal model. Mol Genet Genomics 288(5-6):207-229.

Naruse H, Ishiura H, Mitsui J, Takahashi Y, Matsukawa T, Sakuishi K, Nakamagoe K, Miyake Z, Tamaoka A, Goto J, Yoshimura J, Doi K, Morishita S, Toda T, Tsuji S (2021) Splice-site mutations in KIF5A in the Japanese case series of amyotrophic lateral sclerosis. Neurogenetics 22:11-17.

Niclas J, Navone F, Hom-Booker N, Vale RD (1994) Cloning and localization of a conventional kinesin motor expressed exclusively in neurons. Neuron 12:1059-1072.

Nicolas A, Kenna KP, Renton AE, Ticozzi N, Faghri F, Chia R, Dominov JA, Kenna BJ, Nalls MA, Keagle P, Rivera AM, van Rheenen W, Murphy NA, van Vugt JJFA, Geiger JT, Van der Spek RA, Pliner HA, Shankaracharya, Smith BN, Marangi G, et al. (2018) Genome-wide analyses identify KIF5A as a novel ALS gene. Neuron 97:1268-1283.e6.

Ott B, Dahlke C, Meller K, Napirei M, Schmitt-John T, Brand-Saberi B, Theiss C, Saberi D (2015) Implementation of a manual for working with wobbler mice and criteria for discontinuation of the experiment. Ann Anat 200:118-124.

Ott B, Dahlke C, Saberi D, Brand-Saberi B, Matschke V, Schmitt-John T, Theiss C (2017) Morphological studies of wobbler mouse dorsal root ganglia show neurofilamental disorders. J Neurol Exp Neurosci 3:1-7.

Pernas-Alonso R, Perrone-Capano C, Volpicelli F, di Porzio U (2001) Regionalized neurofilament accumulation and motoneuron degeneration are linked phenotypes in wobbler neuromuscular disease. Neurobiol Dis 8:581-589.

Röderer P, Klatt L, John F, Theis V, Winklhofer KF, Theiss C, Matschke V (2018) Increased ROS level in spinal cord of wobbler mice due to Nmnat2 downregulation. Mol Neurobiol 55:8414-8424.

Rohm M, May C, Marcus K, Steinbach S, Theis V, Theiss C, Matschke V (2019) The microRNA miR-375-3p and the tumor suppressor NDRG2 are involved in sporadic amyotrophic lateral sclerosis. Cell Physiol Biochem 52:1412-1426.

Saberi D, Ott B, Dahlke C, Matschke V, Schmitt-John T, Theiss C (2016) The spatiotemporal pattern of degeneration in the cerebellum of the wobbler mouse. J Neuropathol Exp Neurol 75:347-357.

Schmitt-John T, Drepper C, Mussmann A, Hahn P, Kuhlmann M, Thiel C, Hafner M, Lengeling A, Heimann P, Jones JM, Meisler MH, Jockusch H (2005) Mutation of Vps54 causes motor neuron disease and defective spermiogenesis in the wobbler mouse. Nat Genet 37:1213-1215.

Smith EF, Shaw PJ, De Vos KJ (2019) The role of mitochondria in amyotrophic lateral sclerosis. Neurosci Lett 710:132933.

Stein J, Walkenfort B, Cihankaya H, Hasenberg M, Bader V, Winklhofer KF, Röderer P, Matschke J, Theiss C, Matschke V (2021) Increased ROS-dependent fission of mitochondria causes abnormal morphology of the cell powerhouses in a murine model of amyotrophic lateral sclerosis. Oxid Med Cell Longev 2021:6924251.

Sun Q, Zhao X, Li S, Yang F, Wang H, Cui F, Huang X (2020) CSF neurofilament light chain elevation predicts ALS severity and progression. Front Neurol 11:919.

Taylor JP, Brown RH Jr, Cleveland DW (2016) Decoding ALS: from genes to mechanism. Nature 539:197-206.

Uchida A, Alami NH, Brown A (2009) Tight functional coupling of kinesin-1A and dynein motors in the bidirectional transport of neurofilaments. Mol Biol Cell 20:4997-5006.

Wang Q, Tian J, Chen H, Du H, Guo L (2019) Amyloid beta-mediated KIF5A deficiency disrupts anterograde axonal mitochondrial movement. Neurobiol Dis 127:410-418.

Xia CH, Roberts EA, Her LS, Liu X, Williams DS, Cleveland DW, Goldstein LS (2003) Abnormal neurofilament transport caused by targeted disruption of neuronal kinesin heavy chain KIF5A. J Cell Biol 161:55-66.

Xu GP, Dave KR, Moraes CT, Busto R, Sick TJ, Bradley WG, Pérez-Pinzón MA (2001) Dysfunctional mitochondrial respiration in the wobbler mouse brain. Neurosci Lett 300:141-144.

Yuan A, Rao MV, Veeranna, Nixon RA (2012) Neurofilaments at a glance. J Cell Sci 125(Pt 14):3257-3263.

Yuan A, Rao MV, Veeranna, Nixon RA (2017) Neurofilaments and neurofilament proteins in health and disease. Cold Spring Harb Perspect Biol 9:a018309.

Zou ZY, Zhou ZR, Che CH, Liu CY, He RL, Huang HP (2017) Genetic epidemiology of amyotrophic lateral sclerosis: a systematic review and meta-analysis. J Neurol Neurosurg Psychiatry 88:540-549.

Zwilling M, Theiss C, Matschke V (2020) Caffeine and NAD+ improve motor neural integrity of dissociated wobbler cells in vitro. Antioxidants (Basel) 9:460.

C-Editor: Zhao M; S-Editor: Li CH; L-Editor: Song LP; T-Editor: Jia Y

Additional Figure 1 Multiple sequence alignment of WT, WR, and published Kif5α sequence NM_001039000.4.

Total RNA from the cervical spinal cord of WT and WR animals was isolated and reverse transcribed. cDNA was sequenced with appropriate primers described in methods section. Multiple sequence alignment was performed with MView 1.63. There was no difference in the sequence of Kif5α between homozygous wild-type and wobbler sequences.
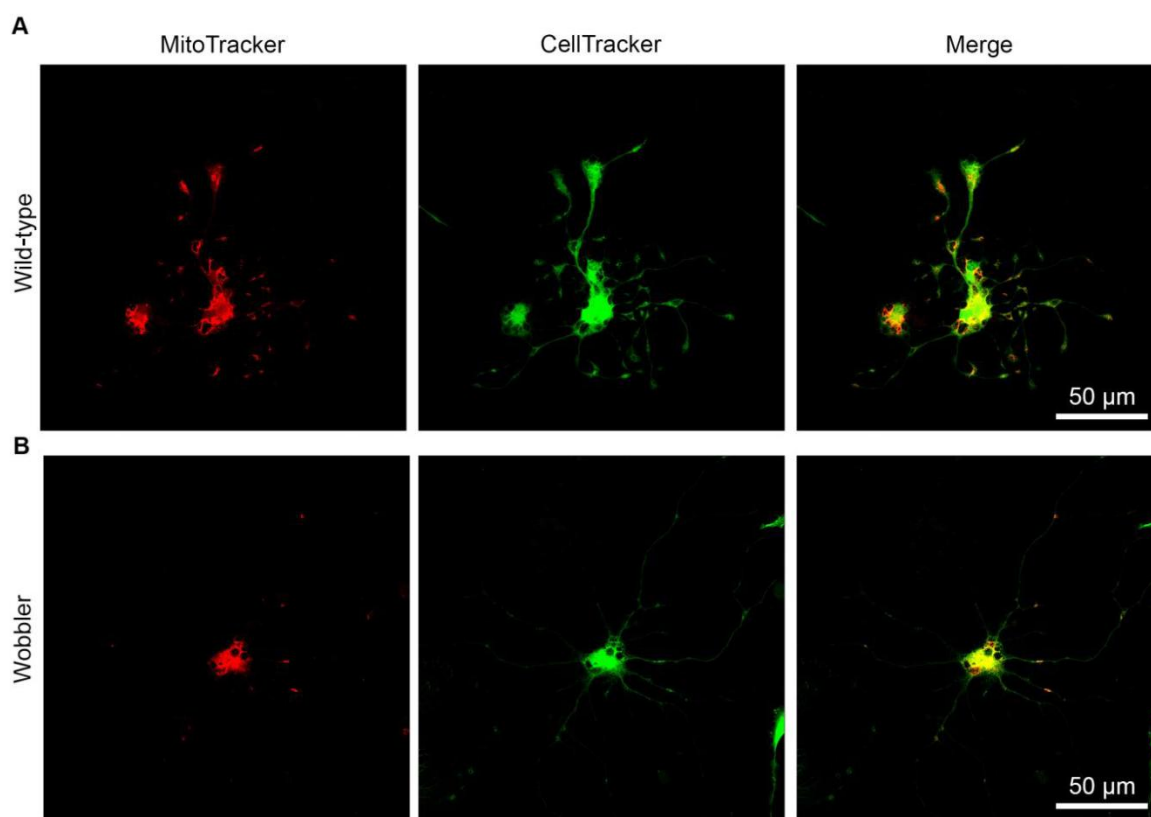
Additional Figure 2 Altered distribution of mitochondria in motor neuronal neurites of wobbler mice.
Exemplary immunofluorescence images of motor neurons in dissociated cell culture of the ventral horn of the spinal cord of WT (A) and WR (B) mice after 10 days in vitro. Staining was performed with CellTracker (green) and MitoTracker (red). Regular accumulations along the neurites were observed in wild-type mice. Wobbler cells showed much less mitochondrial signal, not reaching the distal ends of the branches compared with wild-type cells. Imaging was performed using an inverted confocal Laser Scanning Microscope (LSM 800, Carl Zeiss Microscopy GmbH, Jena, Germany) equipped with the respective filter sets in combination with a 40× objective (Plan-Apochromat 40×/1.4 Oil, Carl Zeiss Microscopy GmbH). White arrowheads indicate MitoTracker signals.